

X-ray diffraction analysis of ZnS/ZnSe superlattices prepared by hot wall epitaxy

Yong Dae Choi, A. Ishida* and H. Fujiyasu*

Department of Physics, Mokwon University, Taejon 301-729, Korea

** Faculty of Engineering, Shizuoka University, Johoku 3-5-1, Hamamatsu 432, Japan*

열벽적층성장 에 의하여 제작된 ZnS/ZnSe 초격자의 X-선 회절분석

최용대, A. Ishida*, H. Fujiyasu*

목원대학교 물리학과, 대전, 301-729

*静岡大學 電子工學科, 浜松, 432, 日本

Abstract ZnS/ZnSe superlattices were prepared on GaAs (100) substrates by hot wall epitaxy, and the structures were analyzed using x-ray diffraction. It is shown that the x-ray diffraction of the strained superlattice gives very useful information about the thickness of each layer, strain, interdiffusion, and the fluctuation of the superlattice period. Interdiffusion length of the S and Se is estimated to be less than 2 Å.

요약 ZnS/ZnSe 초격자가 열벽적층성장 에 의하여 GaAs(100) 기판 위에 성장되었으며 그 구조가 x-선 회절에 의하여 분석되었다. 변형된 초격자의 x-선 회절은 각 층의 두께, 변형, 상호확산 그리고 초격자 주기의 변동에 대한 유용한 정보를 제공한다. S와 Se의 상호확산의 길이는 2Å 이하인 것으로 추정된다.

1. Introduction

ZnSe and ZnS are promising material for

light emitting devices of visible region. Recently the p-type films of the ZnSe or ZnS_{0.5}Se_{0.5} have been prepared using nitrogen

doping, and the possibility of diode laser with blue emission have been increased [1-4]. ZnS/ZnSe superlattices are also useful materials for the devices, and have been studied [5-9]. The superlattice has type-I structure, and shows intense excitonic emission, especially for the sample with thin ZnSe layer [5].

Structural analysis of the superlattice is very important in the research of physical properties and device application. X-ray analysis is one of the most important method to investigate the superlattice structure, especially for the analysis of the strained layer superlattice [10,11]. The x-ray analysis gives very useful and exact information about the superlattice structure, strain, interdiffusion of the constituents, and also about the fluctuation of the superlattice period.

In this study, the structures of ZnS/ZnSe superlattice grown by hot wall epitaxy (HWE) are reported by the analysis of x-ray diffraction pattern. These results are compared with the theoretical calculation data taking into account the strain of the layers.

2. Theory

We now consider the x-ray diffraction from the ZnS/ZnSe superlattice. Figure 1 shows the superlattice structure and strain in the superlattice (SL) schematically. We represent the numbers of atomic layers in ZnS and ZnSe layers as N_A and N_B ,

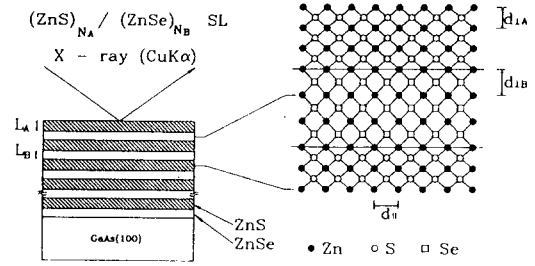


Fig. 1. Schematic superlattice structure and the strain in the superlattice.

respectively and lattice spacings perpendicular to the superlattice layer as d_A and d_B , respectively. X-ray diffraction peaks appear near the angle θ where the equation $2D \sin \theta = n\lambda$ (n : integer, D : superlattice period) is satisfied. The deviation of the peak from the calculated angle is generally small, but it becomes relatively large for the superlattices with broad diffraction peaks. Diffraction intensities can be calculated using the equation below :

$$I = \left\{ F_A \frac{1 - \exp(i4\pi L_A \sin \theta / \lambda)}{1 - \exp(i4\pi d_A \sin \theta / \lambda)} + F_B \exp(i4\pi L_A \sin \theta / \lambda) \right. \\ \left. \frac{1 - \exp(i4\pi L_B \sin \theta / \lambda)}{1 - \exp(i4\pi d_B \sin \theta / \lambda)} \right\}^2 \quad (1)$$

where F_A and F_B are the scattering factors from ZnS and ZnSe layers, respectively, and L_A and L_B are layer thicknesses represented by $N_A d_A$ and $N_B d_B$, respectively. Each scattering factor can be represented using scattering factors of Zn, S and Se layers. To calculate relative peak intensities we used the scattering factors calculated from the

following equations :

$$\begin{aligned} F_A &= f_{zn} + f_s \exp(i2\pi d_{-A} \sin \theta / \lambda) \\ F_B &= f_{zn} + f_{sc} \exp(i2\pi d_{-B} \sin \theta / \lambda) \end{aligned} \quad (2)$$

The lattice constant d_{-i} ($i = A$ or B) of the superlattice is calculated from the parallel lattice spacing $d_{||}$ and unstrained lattice spacing d_i ($i = A$ or B) :

$$d_{-i} = d_i - \frac{2C_{12}^i}{C_{11}^i} (d_{||} - d_i) \quad (3)$$

The $d_{||}$ of the superlattices may be written as below :

$$d_{||} = \frac{G_A L_A d_A + G_B L_B d_B}{G_A L_A + G_B L_B} \quad (4)$$

where G_i ($i = A$ or B) is the value represented as :

$$G_i = C_{11}^i + C_{12}^i - \frac{2(C_{12}^i)^2}{C_{11}^i} \quad (i = A, B) \quad (5)$$

For the ZnS $C_{11}^A = 10.5 \times 10^{11}$ dyn/cm² and $C_{12}^A = 6.53 \times 10^{11}$ dyn/cm², on the other hand, $C_{11}^B = 8.50 \times 10^{11}$ dyn/cm² and $C_{12}^B = 5.02 \times 10^{11}$ dyn/cm² for the ZnSe. So the ratio of the values G_A/G_B becomes 1.17. Real lattice spacing may be somewhat differ from the value calculated above owing to the strain from the substrates or other influences. We used $d_{||}$ as a fitting parameter introducing Δ in the Eq.(4) using the equation below :

$$d_{||} = (1 + \Delta) \frac{1.17L_A d_A + L_B d_B}{1.17L_A + L_B} \quad (6)$$

Strain from the substrate deviates the lattice

spacing parallel to the layer, which somewhat deviates the superlattice period D and also diffraction angles according to $2D \sin \theta = n\lambda$.

When interdiffusion of the constituents is taken into account, the lattice constants and scattering factors vary with the position according to the composition variation. Diffusion from a interface is written as $(1/2)\text{erfc}(z - z_0)/\sqrt{Dt}$ (D : diffusion constant) using the error function complement [10]. In the discussion of the diffusion is independent of the depth (growth time), and defined the \sqrt{Dt} as diffusion length.

3. Experiment

HWE is a convenient method to make not only high quality compound semiconductor films, but also superlattices [5,8]. ZnS/ZnSe superlattices were grown on Cr-doped semi-insulating GaAs (100) substrates using a model FHW 8700 (FUJI SEIKI Inc.) system. Figure 2 shows a schematic diagram of HWE system to prepare ZnS/ZnSe superlattice layer. The system consists of two independent hot wall (HW) furnaces for growing ZnS and ZnSe layer. Figure 3 shows the cross section of the HW furnaces. For the preparation of ZnS/ZnSe superlattices, the substrate was moved onto the outlet of each furnace.

For the growth of ZnS and ZnSe layer, the growth-interruption process was used [12]. This method means that the alternate ZnS and ZnSe layers are grown on GaAs

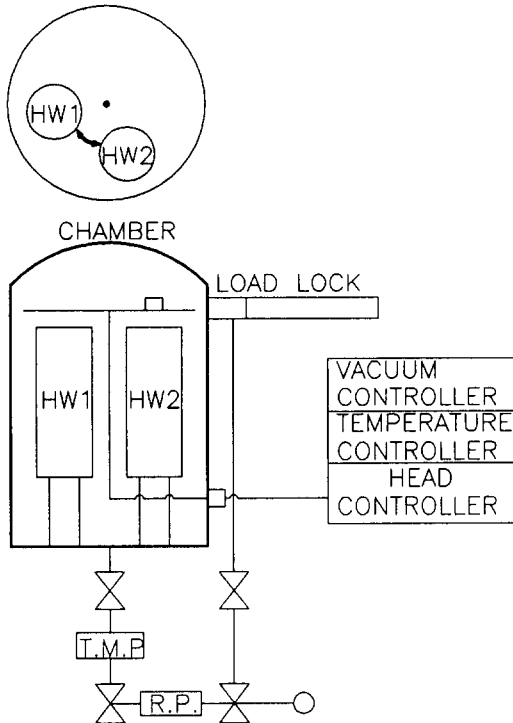


Fig. 2. Schematic diagram of HWE system to prepare ZnS/ZnSe superlattices layer. Two HW furnaces are set on a concentric circle as shown in the left side.

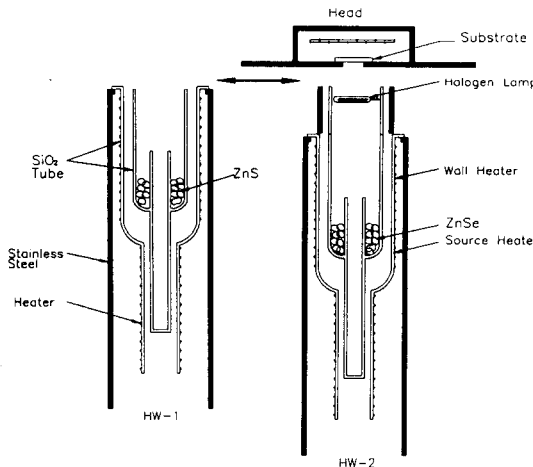


Fig. 3. Cross-section of the HW furnaces used to prepare ZnS/ZnSe superlattices.

substrate successively. In this experiment unlike the conventional method, the wall temperature of the furnace for the growing ZnSe layers was controlled by both the heater wire and halogen lamps. Halogen lamps greatly affected the growth rate and the morphology of ZnSe layers, and were installed to obtain photons to get high quality films. Polycrystalline ZnS and ZnSe as the source material of superlattices were used. The substrates were cleaned by solvent, etched in $\text{H}_2\text{SO}_4 : \text{H}_2\text{O} : \text{H}_2\text{O}_2 = 4 : 1 : 1$, rinsed with deionized H_2O . They were thermally cleaned at 600°C for 10 minutes at a pressure of $\sim 10^{-7}$ torr to remove the remaining oxide layer. During the growth the substrate temperature was kept at 280°C , while the wall and source temperature of ZnSe furnace were 660°C , respectively. Also, the wall and source temperature of ZnS source were 650°C and 700°C , respectively. The thickness of the growing period layer was adjusted by controlling the growing time, using the basic growth rate data of ZnS and ZnSe monolayers. The growth rates of ZnS and ZnSe layer were almost $0.7 \text{ \AA}/\text{sec}$ and $2 \text{ \AA}/\text{sec}$, respectively.

ZnS/ZnSe superlattice structures were ascertained by observing X-ray diffraction satellites. Cu ($K_{\alpha 1}$, $K_{\alpha 2}$) radiation was used for the X-ray source.

4. Results and discussion

ZnS/ZnSe superlattices were prepared by hot wall epitaxy. Figure 4 shows a X-ray

diffraction pattern of a ZnS/ZnSe superlattice and theoretical patterns of $(\text{ZnS})_6/(\text{ZnSe})_{17}$ superlattice with 6 monolayers of ZnS and 17 monolayers of ZnSe without and with diffusion. For the Fig. 4 (b), no diffusion was taken into account, on the other hand, interdiffusion of 2 Å in the length was assumed for the Fig. 4 (c). The superlattice period can be determined accurately from the diffraction peak positions, and thickness of each layers and diffusion can be estimated so that the diffraction intensities fit to the experimental values. In our calculation we assumed that thickness of each layers and the period are integral multiples of the perpendicular lattice spac-

ings. Real superlattice is not always represented by the integral multiple, and spacing of the peak positions sometimes deviates from the calculated values. Uniform deviation of the theoretical peak positions from the experimental values are also occurred by the misestimation of thickness or perpendicular lattice spacing of each layer. In the calculation of this sample we used $\Delta = +0.003$ which gives good agreement between experimental and theoretical peak positions. The positive value of the Δ means that the superlattice layers have tensile strain from the GaAs (100) substrate.

Figure 5 shows the theoretical diffraction patterns of the superlattice $(\text{ZnS})_5/(\text{ZnSe})_{18}$,

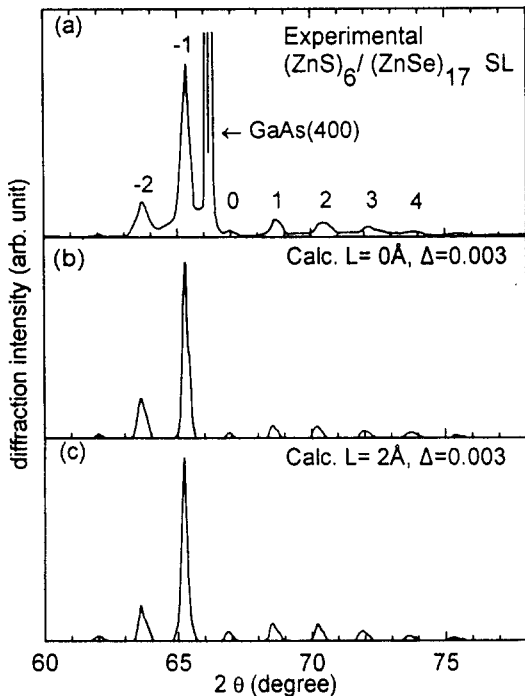


Fig. 4. Experimental and theoretical diffraction patterns of the $(\text{ZnS})_6/(\text{ZnSe})_{17}$ superlattices.

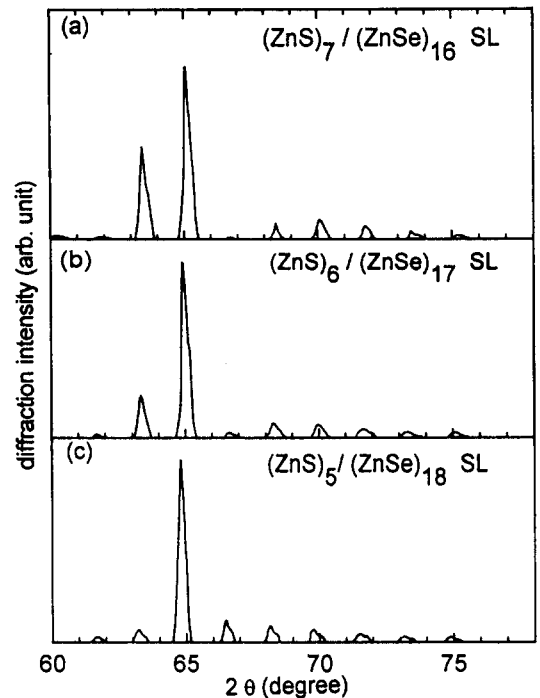


Fig. 5. Theoretical diffraction patterns of $(\text{ZnS})_5/(\text{ZnSe})_{18}$, $(\text{ZnS})_6/(\text{ZnSe})_{17}$ and $(\text{ZnS})_7/(\text{ZnSe})_{16}$ superlattices.

$(\text{ZnS})_6/(\text{ZnSe})_{17}$ and $(\text{ZnS})_7/(\text{ZnSe})_{16}$ without diffusion, and assuming $\Delta = 0$. It is seen that the diffraction peak intensities vary very sensitively with the superlattice structure, and the calculated pattern of Fig. 5 (b) is similar with the experimental pattern in the Fig. 4 (a). However peak positions somewhat differ from the experimental ones. Thus X-ray diffraction gives very useful information determining the thickness of each layer and strain in the strained layer superlattices.

Figure 6 also shows experimental and theoretical X-ray diffraction patterns of $(\text{ZnS})_4/(\text{ZnSe})_8$ superlattice. For the superlattice with relatively short period, diffraction in-

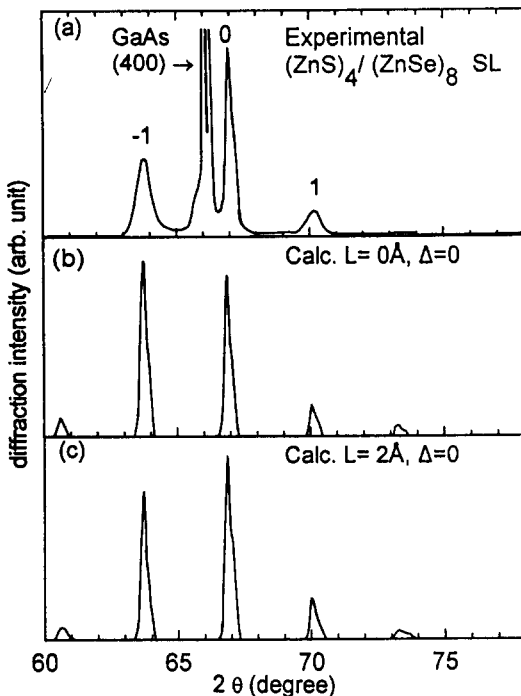


Fig. 6. Experimental and theoretical diffraction patterns of the $(\text{ZnS})_4/(\text{ZnSe})_8$ superlattice.

tensities can be fitted to the experimental pattern better than that of no diffusion as shown in the Fig. 6. In the figure, it should be noted that the experimental diffraction intensities must be compared with theoretical ones by integrated intensities because the full width of half maxima of the diffraction peaks significantly differ peak by peak.

Table 1 shows relative integrated intensities of the experimental and theoretical X-ray diffraction peaks of the various ZnS/ZnSe superlattices. The $(\text{ZnS})_{18}/(\text{ZnSe})_3$ superlattice shown in (d) was grown on ZnS buffer and the others were grown directly on GaAs (100) substrates. In theoretical calculations, two kinds of results were shown: One is without diffusion ($L = 0 \text{ \AA}$) and the other with diffusion of 2 \AA in the diffusion length ($L = 2 \text{ \AA}$). The agreement of the theoretical intensities with the experimental ones is better in $L = 2 \text{ \AA}$ than in $L = 0 \text{ \AA}$. Thus the interdiffusion length of the superlattice is estimated to be as large as 2 \AA . However, the calculated diffusion length may give real diffusion length directly.

Figure 7 shows a model of the fluctuation or imperfection of the ZnS/ZnSe interface and resultant lattice spacing distribution. If there are atomic steps shown in the figure, the lattice spacing at the interface deviates and the diffraction intensities becomes similar to the interdiffusion. Thus real diffusion is considered to be smaller than the value calculated. In any case, it is concluded that the interdiffusion of these ZnS/ZnSe superlattices prepared by hot wall epitaxy is

Table 1

Experimental and theoretical X-ray diffraction intensities of the various ZnS/ZnSe superlattices

(a) (ZnS) ₆ /(ZnSe) ₁₇ SL								$\Delta = +0.003$	1.9 μm (thickness)
Index	- 2	- 1	0	+ 1	+ 2	+ 3	+ 4		
Exp.	0.27	1	0.043	0.086	0.10	0.070	0.032		
Calc. (L = 0 Å)	0.24	1	0.042	0.089	0.08	0.055	0.036		
Calc. (L = 2 Å)	0.21	1	0.052	0.12	0.10	0.059	0.027		
(b) (ZnS) ₄ /(ZnSe) ₈ SL								$\Delta = 0$	0.3 μm
Index	- 2	- 1	0	+ 1	+ 2	+ 3	+ 4		
Exp.	—	0.75	1	0.2	0.024	—	—		
Calc. (L = 0 Å)	0.12	1.1	1	0.23	0.082	—	—		
Calc. (L = 2 Å)	0.078	0.81	1	0.22	0.035	—	—		
(c) (ZnS) ₁₆ /(ZnSe) ₄ SL								$\Delta = 0$	1 μm
Index	- 3	- 2	- 1	0	+ 1	+ 2	+ 3		
Exp.	0.12	0.30	—	0.63	1	0.08			
Calc. (L = 0 Å)	0.11	0.17	0.26	0.46	1	0.024			
Calc. (L = 2 Å)	0.11	0.22	0.38	0.65	1	0.029			
(d) (ZnS) ₁₈ /(ZnSe) ₃ SL								$\Delta = - 0.001$	0.7 μm (including ZnS buffer)
Index	- 3	- 2	- 1	0	+ 1	+ 2	+ 3		
Exp.	—	—	—	1	0.84	—	—		
Calc. (L = 0 Å)	—	0.12	0.25	1	1.06	0.011	—		
Calc. (L = 2 Å)	—	0.12	0.26	1	0.75	0.008	—		

very small and the diffusion length is less than 2 Å. It is also observed that the (ZnS)₁₈/(ZnSe)₃ superlattice grown on ZnS buffer has compressive strain from the ZnS buffer by about 0.1 % as shown in Table 1

(d). This strain is due to the small lattice spacing difference between ZnS and the superlattice of only 0.8 %.

The full width at half maximum of the X-ray diffraction peak gives a useful informa-

Table 2

Deviation of X-ray diffraction peak positions of $(\text{ZnS})_6/(\text{ZnSe})_{17}$ SL by monolayer deviation of the ZnSe layer maintaining one period layers to 23 (a) and maintaining ZnS layers to 6 (b), and experimental full widths of half maxima of the diffraction peaks

Index		- 2	- 1	0	+ 1	+ 2	+ 3
(a) deviation	(deg.)	0.13	0.13	0.14	0.14	0.15	0.15
(b) deviation	(deg.)	0.11	0.04	0.04	0.12	0.18	0.26
FWHM	(deg.)	0.30	0.19	0.17	0.20	0.30	0.45

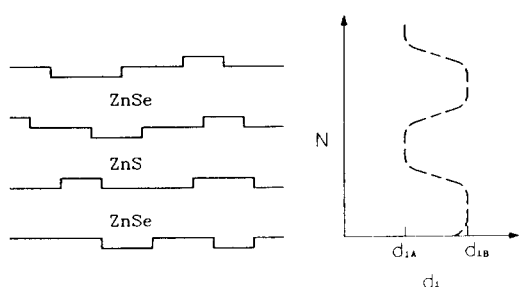


Fig. 7. A model of the fluctuation of the interface, which gives similar influence on the X-ray diffraction pattern of the superlattice with the interdiffusion of the constituents.

tion about the fluctuation of the period. Table 2 shows the deviation of the peak positions in the $(\text{ZnS})_6/(\text{ZnSe})_{17}$ superlattice by monolayer deviation of the ZnSe layer thickness and full width at half maxima (FWHM) of the experimental peaks. The (a) and (b) in the table show monolayer deviation of the ZnSe layer with and without keeping one-period layer number, respectively. It is observed that the FWHM increases with increasing the absolute value of the diffraction index, according with the theoretical values in (b). This is due to the

fluctuation of superlattice period. Though the determination of the amount of the fluctuation need deeper consideration, it seems that 30~40 % in the $(\text{ZnS})_6/(\text{ZnSe})_{17}$ superlattice consists of more or less than 23 monolayers in one period.

5. Conclusion

ZnS/ZnSe superlattices were prepared by hot wall epitaxy and superlattice structure were analyzed by X-ray diffraction. It was shown that the X-ray diffraction gives useful information about the thickness of each layer, strain, interdiffusion, and fluctuation of the superlattice layers. The lattice mismatch of the ZnS and ZnSe was completely accommodated by the lattice strain, and the interdiffusion length of the S and Se was less than 1 monolayer. It is also observed that the superlattice layer was strained by the GaAs (100) substrate or ZnS buffer layer when the parallel lattice spacing becomes close to the lattice spacing of the substrate or the buffer.

Acknowledgements

One of the authors, Y.D. Choi, wishes to acknowledge KOSEF for financial support to perform this work.

References

- [1] M.A. Hasse, J. Qiu, J.M. Depuydt and Cheng, *Appl. Phys. Lett.* 59 (1991) 1272.
- [2] R.N. Bhargava, *J. Cryst. Growth* 59 (1982) 15.
- [3] K. Ohkawa, T. Karasawa and T. Mitsuyu, *Jpn. J. Appl. Phys.* 30, L152 (1991).
- [4] S. Itoh, N. Nakayama, S. Matsumoto, M. Nagai, K. Nakano, M. Ozawa, H. Okuyama, S. Tomiya, T. Toyoharu, M. Ikeda, A. Ishibashi and Y. Mori, *Jpn. J. Appl. Phys.* 33, L938 (1994).
- [5] H. Fujiyasu, H. Takahashi, H. Shimizu, A. Sasaki and H. Kuwabara, *Proc. of 17th Int. Conf. on Physics of Semiconductors*, San Francisco (1984) 559.
- [6] T. Yokogawa, M. Ogura and T. Kajiwara, *Appl. Phys. Lett.* 49 (1986) 1702.
- [7] A. Taike, N. Teraguchi and M. Konagai, *Jpn. J. Appl. Phys.* 26, L989 (1987).
- [8] S. Sakakibara, K. Fujimoto, N. Amano, K. Ishino, A. Ishida and H. Fujiyasu, *Jpn. J. Appl. Phys.* 33 (1994) 2008.
- [9] H. Fujiwara, H. Kiryu and I. Shimizu, *J. Appl. Phys.* 77(8) (1995) 3927.
- [10] A. Ishida, M. Aoki and H. Fujiyasu, *J. Appl. Phys.* 58 (1985) 797.
- [11] A. Segm ller and A.E. Blakeslee, *J. Appl. Crystallogr.* 6, 19 (1973).
- [12] H. Fujiyasu, A. Ishida, H. Kuwabara, S. Shimomura, S. Takaoka and K. Murase, *Surf. Sci.* 142 (1984) 579.